ORIGINAL ARTICLE

The Nucleus Accumbens CRH–CRHR1 System Mediates Early-Life Stress-Induced Sleep Disturbance and Dendritic Atrophy in the Adult Mouse

Ting Wang[1] · Yu-Nu Ma[1] · Chen-Chen Zhang[1] · Xiao Liu[1] · Ya-Xin Sun[1] · Hong-Li Wang[1] · Han Wang[1] · Yu-Heng Zhong[2] · Yun-Ai Su[1] · Ji-Tao Li[1] · Tian-Mei Si[1]

Abstract Adverse experiences in early life have long-lasting negative impacts on behavior and the brain in adulthood, one of which is sleep disturbance. As the corticotropin-releasing hormone (CRH)–corticotropin-releasing hormone receptor 1 (CRHR1) system and nucleus accumbens (NAc) play important roles in both stress responses and sleep-wake regulation, in this study we investigated whether the NAc CRH–CRHR1 system mediates early-life stress-induced abnormalities in sleep-wake behavior in adult mice. Using the limited nesting and bedding material paradigm from postnatal days 2 to 9, we found that early-life stress disrupted sleep-wake behaviors during adulthood, including increased wakefulness and decreased non-rapid eye movement (NREM) sleep time during the dark period and increased rapid eye movement (REM) sleep time during the light period. The stress-induced sleep disturbances were accompanied by dendritic atrophy in the NAc and both were largely reversed by daily systemic administration of the CRHR1 antagonist antalarmin during stress exposure. Importantly, *Crh* overexpression in the NAc reproduced the effects of early-life stress on sleep-wake behavior and NAc morphology, whereas NAc *Crhr1* knockdown reversed these effects (including increased wakefulness and reduced NREM sleep in the dark period and NAc dendritic atrophy). Together, our findings demonstrate the negative influence of early-life stress on sleep architecture and the structural plasticity of the NAc, and highlight the critical role of the NAc CRH–CRHR1 system in modulating these negative outcomes evoked by early-life stress.

Keywords Early-life stress · Sleep · CRH–CRHR1 · Nucleus accumbens · Morphology

✉ Ji-Tao Li
ljt_102124@163.com

✉ Tian-Mei Si
si.tian-mei@163.com

1 Peking University Sixth Hospital, Peking University Institute of Mental Health, NHC Key Laboratory of Mental Health (Peking University), National Clinical Research Center for Mental Disorders (Peking University Sixth Hospital), Beijing 100191, China

2 Department of Pharmacology, School of Basic Medical Sciences, State Key Laboratory of Medical Neurobiology and MOE Frontiers Center for Brain Science, Institutes of Brain Science, Fudan University, Shanghai 200032, China

Introduction

Stressful experiences during the early postnatal period have long-lasting negative impacts in later life [1–3], such as sleep disturbance in adulthood (e.g., insomnia and poor sleep quality) [4–9]. Animal studies have also reported the negative effects of early-life stress on sleep-wake behavior (mainly using the maternal separation paradigm) [10]. For instance, it has been consistently found that early-life stress increases rapid-eye-movement (REM) sleep during the inactive period [11–15]. With the animal models, it is now plausible to examine in depth the mechanisms underlying the sleep disturbances induced by early-life stress, the understanding of which have important implications in the treatment and prevention of stress- and sleep-related disorders.

Accumulating evidence highlights that corticotropin-releasing hormone (CRH), acting through its type 1 receptor (CRHR1), is a key mediator of the negative impact of early-life stress on behavior and the brain. For

example, systemic administration of the CRHR1 antagonist antalarmin during early-life stress exposure prevents stress-induced cognitive impairments (e.g., spatial memory [16–18] and temporal order memory [17, 19]) and neuronal structural atrophy in the mouse medial prefrontal cortex and hippocampus in adulthood [16, 19]. On the other hand, the CRH–CRHR1 system has been found to regulate the sleep-wake cycle [10, 20, 21]. For example, long-term overexpression of CRH in mice promotes REM sleep [22]. Intracerebroventricular (ICV) administration of CRH in rats increases wakefulness [23] and decreases non-rapid-eye-movement (NREM) and REM sleep [24]. It is thus possible that the CRH–CRHR1 system mediates early-life stress-induced sleep disturbances.

The nucleus accumbens (NAc) is one of the critical brain regions where stress responses and sleep regulation may interact. As a key node in the brain reward circuitry [25], the NAc has been increasingly recognized for its role in sleep-wake regulation [26, 27]. Lesions of the NAc by ibotenic acid increase the total time spent awake and reduce the mean duration per episode of NREM sleep [28]. We have previously shown that early-life stress-induced sleep alterations in aged mice are accompanied by excitatory-inhibitory imbalance in the NAc [29]. As CRH and its type 1 receptor CRHR1 is widely expressed in the NAc [30], and CRH-expressing neurons have been found in this area [31], we hypothesized that the CRH–CRHR1 system in the NAc may be involved in the sleep-wake abnormalities induced by early-life stress.

In this study, we carried out four experiments to test the mediating role of the NAc CRH–CRHR1 system in the effects of early-life stress on sleep-wake behavior in adulthood. We adopted a naturalistic mouse model of early-life stress, the limited nesting and bedding material procedure [18, 32], and examined the sleep-wake behavior in adult mice *via* electroencephalogram (EEG)/electromyogram (EMG) polysomnographic recordings. We also examined the effects of early-life stress on dendritic structure in the NAc, as our previous studies have consistently demonstrated the deleterious effects of early-life stress on structural plasticity in cortical regions [19, 33]. We then investigated whether the effects of early-life stress on sleep-wake behavior and NAc morphology could be prevented by systemic CRHR1 blockade (*via* antalarmin treatment). Finally, using viral microinjection, we determined whether the effects of early-life stress on sleep-wake behavior and NAc morphology could be reproduced by *Crh* overexpression or prevented by *Crhr1* knockdown in the NAc to confirm the involvement of the NAc CRH–CRHR1 system in early-life stress effects.

Materials and Methods

Animals

Adult male and female C57BL/6N mice were obtained from Vital River Laboratories (Beijing, China) for breeding. After habituation, each female was housed with one male for 2 weeks and then singly housed. The pregnant females were monitored daily for pup delivery, and the day of parturition was defined as postnatal day 0 (PND0). Only male offspring were used for experiments. CRH-Cre mice were from The Jackson Laboratory (stock number: 012704) and maintained fully back-crossed onto C57BL/6N mice, and adult male heterozygous mice were used.

All mice were maintained under a 12-h light/dark cycle (lights on at 08:00) and constant temperature (23 ± 1°C) in a humidity-controlled (35%–55%) vivarium and had unlimited access to food and water. All procedures were performed in accordance with the National Institute of Health Guide for the Use and Care of Laboratory Animals and were approved by the Peking University Committee on Animal Care and Use.
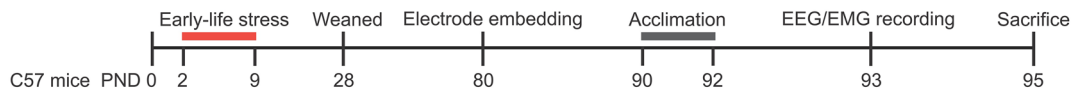
Experimental Design

Four experiments were carried out. In Experiment 1, the effects of early-life stress on sleep-wake behavior and NAc dendritic morphology were examined (Fig. 1A). After the stress procedure (PND9), litters of pups were transferred to standard cages and weaned on PND28. Sleep-wake behaviors were monitored in adulthood (PND93). Mice were then killed (PND95) for Golgi-Cox staining and immunostaining. The expression levels of CRH and CRHR1 [using quantitative reverse transcription PCR (RT-qPCR)] and vesicular transporters of glutamate and γ-aminobutyric acid (GABA) (using immunofluorescence) in the NAc were also measured. Experiment 2 examined the effects of concomitant CRHR1 blockade on early-life stress-induced abnormalities in sleep-wake behavior and NAc dendritic morphology (Fig. 3A). Experiments 3 and 4 evaluated the involvement of the CRH–CRHR1 system in the NAc in the negative effects of early-life stress. In Experiment 3, we over-expressed *Crh* in the NAc to determine whether up-regulating the NAc CRH–CRHR1 system could reproduce the effects of early-life stress (Fig. 4A). In Experiment 4, we investigated whether NAc *Crhr1* knockdown could reverse the negative effects of early-life stress (Fig. 5A).
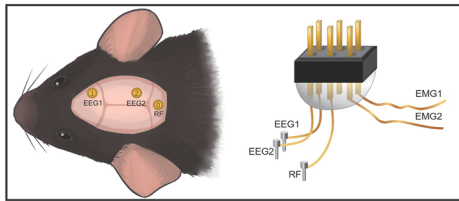
Early-Life Stress Procedure

The limited nesting and bedding material procedure was used as an early-life stressor and carried out as previously described [18, 34]. Briefly, on the morning of PND2, pups
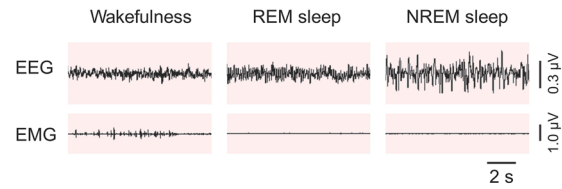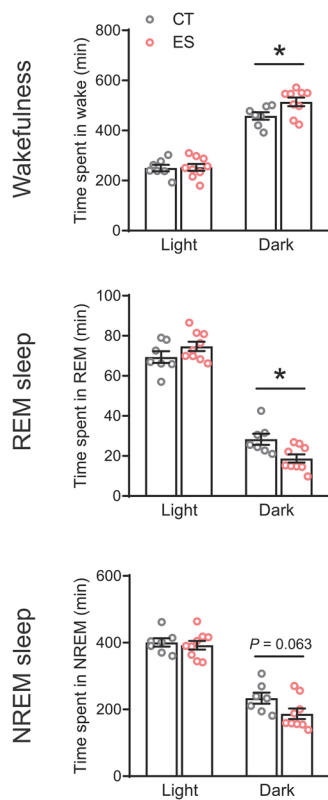
A Experimental design
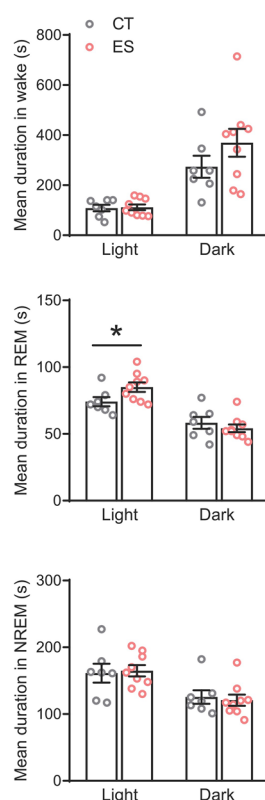

B EEG/EMG surgery and electrode

C Typical examples of EEG and EMG

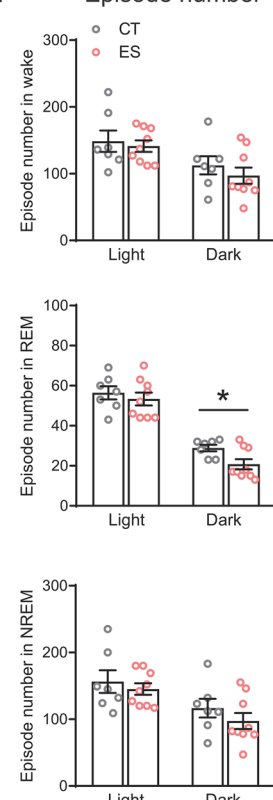## D Total time

E Mean duration

F Episode number

Fig. 1 Effects of early-life stress on sleep-wake behavior in adulthood. **A** Schematic of the design of Experiment 1. **B, C** Electrode embedding sites, electrode preparation, and typical examples of EEG and EMG during wakefulness, REM sleep, and NREM sleep in an adult mouse. **D** Total time spent in wakefulness, REM, and NREM sleep during the light and dark period. Early-life stress increases wakefulness, reduces REM sleep, and tends to reduce NREM sleep during the dark period. **E** Early-life stress increases the mean duration of REM sleep during the light period. **F** Early-life stress reduces the number of REM episodes during the dark period. CT, control; EEG, electroencephalogram; EMG, electromyogram; ES, early-life stress. NREM, non-rapid eye movement; PND, postnatal day; REM, rapid eye movement; RF, reference. *$P < 0.05$; independent-samples *t*-tests; CT: $n = 7$; ES: $n = 9$.

were weighed and litters culled to 6–8 pups including both sexes. Control dams were provided with standard amounts of nesting material [2 squares (4.8 g) of Nestlets (Indulab,

Gams, Switzerland)] and 500 mL sawdust bedding. In the "stress" cages, dams were equipped with a fine-gauge aluminum mesh platform (McNichols, Tampa, USA) with 200

mL of corncob bedding on the bottom for dropping collection. A limited quantity of nesting material [1/2 square (1.2 g) of Nestlets] was placed on top of the mesh. The stress procedure ended on the morning of PND9. Male offspring were weaned on PND28 and group-housed 3–4 per cage for further study.

Drug Treatment

Drugs were administered at 09:00–12:00 on PND2–8. Control and stressed pups received a daily subcutaneous injection of vehicle (15% β-cyclodextrin in sterile normal saline) or antalarmin hydrochloride (20 µg/g body weight; Tocris Bioscience, Bristol, UK). The dosage choice was based on previous studies [19, 33, 35]. Before the injection, the home cage containing the litter was placed on a heating pad maintained at 30–33 °C. The dam was then removed from the litter and transferred to a clean cage. Within each litter, 1–3 male pups were randomly assigned to each drug treatment group. Pups were marked on the paw pads with a marker pen, weighed, and injected with the drug or vehicle (5 µL/g of body weight) into the nape of the neck. The duration of injection was < 15 min per litter. After the injection, the dam was placed back in the home cage and the litter remained undisturbed for the next 24 h.

EEG/EMG Surgical Implantation

Mice were implanted with EEG and EMG electrodes for polysomnographic recordings (Fig. 1B). In Experiments 1 and 2, the implantation was carried out on PND80 according to a previously described procedure [29, 36]. Mice were anesthetized with an intraperitoneal injection of pentobarbital (100 mg/kg). To monitor the EEG, two stainless-steel recording screws were positioned 1 mm anterior to bregma or lambda, both 1.5 mm lateral to the midline. In Experiments 3 and 4 that involved stereotaxic surgery for viral injection, the implantation was carried out on PND75 together with the surgery (see below) and 2 EEG stainless miniature screws were carefully inserted into the holes for virus injection. For all experiments, a reference screw was inserted into the skull above the cerebellum. Stainless steel wires were inserted bilaterally into the trapezius (neck) muscles to record skeletal muscle activity. The EEG/EMG electrodes were fixed to the skull using dental cement. The incision site was closed with non-dissolvable silk sutures and treated with erythromycin ointment on the first day after surgery. Mice were allowed to recover for at least 10 days before they were acclimated to the recording cables.

EEG/EMG Recordings and Analysis

Mice were individually placed in sleep-recording cages for 3-day acclimatization and were allowed relatively unrestricted movement; they were kept in the same lighting and temperature conditions as the cages in the preoperative period. Flexible cables that were mounted to fixed commutators were attached to the electrode pedestals. EEG/EMG signals were then monitored for 24 h, beginning at 08:00.

The EEG/EMG signals were amplified and filtered (EEG: 0.5–30 Hz; EMG: 20–200 Hz), digitized at a sampling rate of 500 Hz, and analyzed using SleepSign software (Kissei Comtec Co., Nagano, Japan). The vigilance states were divided into consecutive non-overlapping 4-s epochs and each epoch was classified as wakefulness, REM sleep, or NREM sleep (Fig. 1C). Wakefulness was identified by high frequency, desynchronized EEG, and frequent EMG activity. REM sleep was identified by theta waves (4–9 Hz) of consistent low amplitude on the EEG recording together with the absence of EMG activity. NREM sleep was identified by the dominant presence of high-amplitude, low frequency (0.5–4 Hz, delta) EEG activity in the absence of motor activity. Vigilance states assigned by SleepSign were examined visually and corrected manually if necessary.

Golgi-Cox Staining and the Analysis of Dendrites and Spines

Brains were dissected and immersed in Golgi-Cox solution [37] for 14 days and then transferred to 30% sucrose for 2–5 days in the dark at room temperature. Serial coronal sections were cut at 120 µm on a Microm HM 650 V vibratome (Thermo Scientific, Walldorf, Germany), mounted on Superfrost plus slides (Thermo Scientific), and processed as described previously [19]. For each mouse, 6–8 fully Golgi-impregnated medium spiny neurons (MSNs) per subregion were randomly chosen. Neurons were traced at 400× with Neurolucida software (MicroBrightField Bioscience, Williston, USA), and Sholl analysis was applied to measure the total dendritic length and the number of intersections at concentric circles (10 µm apart) using NeuroExplorer (MicroBrightField Bioscience) [38].

For the analysis of dendritic protrusions, 6–8 segments of each dendritic domain per subregion were digitized at 1000× using a CoolSNAP MP5 CCD camera (Roper Scientific, Tucson, USA) mounted on an Olympus BX51 microscope (Olympus, Tokyo, Japan). Dendritic protrusions were identified and categorized into three subtypes: (1) thin spines (long and thin protrusions with a bulbous head), (2) mushroom spines (protrusions with a small neck and a large head), and (3) stubby spines (protrusions that closely connect to the dendritic shaft and lack a clear neck) based on established criteria [39]. Dendritic protrusions were counted

manually using NIH ImageJ software (National Institutes of Health, USA), and the data are expressed as the number of protrusions per 10 μm of dendrite.

Immunostaining and Image Analysis

Mice were anesthetized with sodium pentobarbital (200 mg/kg, i.p.) and transcardially perfused with 0.9% saline followed by 4% buffered paraformaldehyde. After post-fixation and cryoprotection, serial coronal sections throughout the NAc (Bregma 1.70–0.86 mm) were cut on a cryostat (Leica, Wetzlar, Germany) at 30 μm thickness and 180 μm intervals.

For immunofluorescence, the sections were rinsed in PB (phosphate buffer), treated with 1% normal donkey serum (1 h), and labeled with rabbit anti-CRH (1:1000, T-4037, BMA Biomedicals, Switzerland), goat anti-CRHR1 (1:50, ab59023, Abcam, Cambridge, UK), mouse anti-VGluT1 (1:1000, Cat. No. 135011, Synaptic Systems, Germany), and rabbit anti-VGAT (1:500, Cat. No. 131013, Synaptic Systems) at 4 °C overnight. The next day, the sections were rinsed three times and labeled with Alexa Fluor 488- and/or 594-conjugated secondary antibodies raised in donkey (1:500; Invitrogen, Carlsbad, USA) at room temperature (2 h). Then the sections were transferred onto slides and covered with Vectashield containing 4′,6-diamidino-2-phenylindole (Vector Laboratories, Burlingame, USA).

For image analysis, brain sections were randomly coded so that investigators were blind to the experimental conditions. Images were acquired from 3 sections per animal at 200× using an Olympus IX81 laser-scanning confocal microscope. NIH ImageJ software was used to quantify the immunoreactivity of CRH, CRHR1, VGluT1, and VGAT. Relative protein levels were determined by the optical density values of subregions subtracted from the corpus callosum, which was regarded as background, and then compared between groups. Images were adjusted for optimal brightness and contrast using FV10-ASW 1.7 software (Olympus).

RNA Extraction and Real-Time Quantitative Reverse Transcription PCR (Real-Time RT-qPCR)

Mice were anesthetized with isoflurane (3% induction) and the NAc was rapidly dissected from the brain on ice. Total RNAs from mouse tissue were extracted using an EasyPure RNA Kit (TransGen Biotech, Beijing, China), and reverse-transcribed (1 μg) with TransScript All-in-One First-Strand cDNA Synthesis SuperMix (TransGen Biotech) according to the manufacturer's instructions. Using corresponding primers (*Crh* or *Crhr1*) and Trans Start Top/Tip Green qPCR SuperMix (TransGen Biotech) on a Real-Time PCR Detection System (Roche, Germany), the qPCR assay was performed under the following conditions: 1 μL forward primer, 1 μL reverse primer, 25 μL 2×

TransStart Top/Tip Green qPCR SuperMix, 1 μL cDNA, and 22 μL distilled water). The reaction conditions were as follows: 95°C for 30 s of initial denaturation, followed by 40 cycles of 95 °C for 5 s and 60 °C for 30 s. The conditions of the dissociation step were as follows: 95 °C for 10 s, 60 °C for 60 s, 95 °C for 1 s, and 37 °C for 30 s. Primers for *Crh*, *Crhr1*, and *Gapdh* were designed according to published NCBI sequences:

Crh: forward 5′-TCTCACCTTCCACCTTCTGC-3′
Crh: reverse 3′-TTCCTGTTGCTGTGAGCTTG-5′
Crhr1: forward 5′-TGCCAGGAGATTCTCAACGAA-3′
Crhr1: reverse 3′-AAAGCCGAGATGAGGTTCCAG-5′
Gapdh: forward 5′-AGGTCGGTGTGAACGGATTTG-3′
Gapdh: reverse 3′-TGTAGACCATGTAGTTGAGGTCA-5′

Viruses

To overexpress *Crh* in the NAc, we used adeno-associated virus (AAV) 2/9 vectors carrying AAV-CAG-DIO-CRH-P2A-GFP (CRH_OE, 3.22×10^{13} particles/mL; Vigene Biosciences, Shandong, China). To achieve *Crhr1* knockdown in the NAc, we applied the lentivirus-mediated short hairpin RNA (shRNA) interference technique. The shRNA sequence for *Crhr1* was 5'-GATCCGGAACATCATCCACTGGAACCTTCAAGAGAGGTTCCAGTGGATGATGTTCCTTTTTTA-3' and the knockdown virus (CRHR1_KD) was pLent-U6-GFP-P2A-shRNA1 (3.20×10^9 particles/mL, Vigene Biosciences). The control viruses for CRH_OE and CRHR1_KD were AAV2/9-CAG-DIO-GFP (3.23×10^{13} particles/mL, Vigene Biosciences) and pLent-U6-GFP-Puro (1.20×10^9 particles/mL, Vigene Biosciences), respectively.

Stereotaxic Surgery and Viral Microinjection

The procedures for stereotaxic surgery and microinjection were as previously described [36]. Mice were anesthetized with isoflurane (3% induction, 1.5% maintenance) and received viral microinjections into the bilateral NAc through a glass micropipette. The injection coordinates (relative to bregma) were anterior +1.4 mm, lateral ±1.0 mm, and ventral −4.0 mm. The viral injection volumes were as follows: AAV: 0.25 μL/hemisphere at a rate of 0.05 μL/min; lentivirus: 1 μL/hemisphere at 0.1 μL/min. After injection, the pipette was left in place for an additional 5 min and then slowly withdrawn. Animals were treated with a topical antibiotic (erythromycin ointment) on the first day after the surgery. Two weeks after surgery, qPCR was carried out to confirm the efficiency of viral transduction. Viral transduction was also verified using fluorescence microscopy.

Statistical Analysis

All data are presented as the mean $\pm$ SEM. SPSS 26.0 software (SPSS, Chicago, USA) and GraphPad Prism 8.0 (GraphPad Software, San Diego, USA) were used for statistical analysis. Comparisons between two groups in Experiments 1 and 3 were carried out using independent-samples t-tests. Comparisons between four groups were carried out using two-way analysis of variance (ANOVA), with stress (control vs early stress) and treatment (vehicle vs antalarmin in Experiment 2; control vs knockdown in Experiment 4) as factors, followed by the Bonferroni $post\ hoc$ test when appropriate. Repeated measures ANOVA was used for the number of dendritic branch points. $P < 0.05$ was considered significant.

Results

Early-Life Stress Disrupts Sleep-Wake Behavior, Induces NAc Dendritic Atrophy, and Up-Regulates NAc CRH–CRHR1 Signaling in Adult Mice

We evaluated the effects of early-life stress on sleep-wake behavior in adulthood by comparing the sleep-wake profiles of adult mice exposed to a limited nesting and bedding material procedure in the early postnatal period (PND2–9) with those of control mice (Fig. S1). For the total time spent in each vigilance state (wakefulness, REM sleep, and NREM sleep; Fig. 1D), early-life stress significantly increased the time spent awake during the dark period ($t_{14} = 2.355$, $P = 0.034$). The increased wakefulness was accompanied by a reduced REM sleep time ($t_{14} = 2.865$, $P = 0.012$) and a tendency of decreased NREM sleep ($t_{14} = 2.022$, $P = 0.063$). The previously-documented increase in REM sleep time during the light period [12–15] was noticeable in this experiment, despite not approaching significance ($t_{14} = 1.445$, $P = 0.170$). When the total time in each state was decomposed into the mean duration per episode (Fig. 1E) and the number of episodes (Fig. 1F), early-life stress increased the mean duration of REM sleep during the light period ($t_{14} = 2.152$, $P = 0.049$) and the number of REM episodes during the dark period ($t_{14} = 2.499$, $P = 0.026$), which contributed to the changes in the total time of REM sleep during the light and dark periods.

We then assessed the effects of early-life stress on the dendritic morphology of NAc neurons in two subregions [core (NAcc) and shell (NAcsh)] using the Golgi-Cox staining method (Fig. 2A, B). Early-life stress significantly reduced the length (NAcc: $t_{12} = 4.192$, $P = 0.001$; NAcsh: $t_{12} = 7.602$, $P < 0.001$) and complexity (NAcc: $F_{1,12} = 36.593$, $P < 0.001$; NAcsh: $F_{1,12} = 29.915$, $P < 0.001$) of dendrites in both NAcc (Fig. 2C) and NAcsh (Fig. 2D). Spine loss was

observed in stressed mice on the thin (NAcc: $t_{12} = 8.671$, $P < 0.001$; NAcsh: $t_{12} = 3.509$, $P = 0.004$) and stubby (NAcc: $t_{12} = 6.015$, $P < 0.001$; NAcsh: $t_{12} = 2.676$, $P = 0.020$) spines in both NAcc (Fig. 2E) and NAcsh (Fig. 2F). The area of the cell body was not significantly affected by early-life stress in either NAcc (Fig. S2A) or NAcsh (Fig. S2B). These results demonstrated that early-life stress simplified dendritic structure and reduced spine density throughout the NAc. Meanwhile, RT-qPCR revealed that the levels of Crh and $Crhr1$ messenger RNA (mRNA) in the NAc were significantly increased in early-life stressed mice (Crh: $t_8 = 3.470$, $P = 0.008$; $Crhr1$: $t_8 = 2.669$, $P = 0.028$; Fig. 2G, H), indicating an up-regulated CRH–CRHR1 signaling system in the NAc following early-life stress.

Using immunofluorescence (Fig. S3A, B) we measured the expression levels of the vesicular transporters of glutamate and GABA in presynaptic terminals, that is, vesicular glutamate transporter-1 (VGluT1) and vesicular GABA transporter (VGAT). These transporters are responsible for loading glutamate and GABA into synaptic vesicles for future release [40] and contribute significantly to the regulation of excitatory-inhibitory neurotransmission [41, 42]. We found that early-life stress down-regulated VGluT1 expression ($F_{1,20} = 8.136$, $P = 0.001$; Fig. S3C, left), up-regulated VGAT expression ($F_{1,20} = 9.132$, $P = 0.007$; Fig. S3C, middle), and reduced the VGluT1/VGAT ratio ($F_{1,20} = 10.80$, $P = 0.004$; Fig. S3C, right) across the two subregions of the NAc, with no significant stress × subregion interaction (all $F < 0.280$, all $P > 0.602$). These results indicate that early-life stress-induced hyperexcitability in the area accompanies the structural deficits we observed above.

CRHR1 Blockade via Antalarmin Treatment Attenuates Early-Life Stress-Induced Sleep Disturbance and NAc Dendritic Atrophy

We then tested the involvement of the CRH–CRHR1 system in the negative effects of early-life stress by determining whether systemic CRHR1 blockade (by concomitant daily administration of the CRHR1 antagonist antalarmin from PND2 to PND9) could attenuate the early-life stress-induced abnormalities in sleep-wake behavior and NAc dendritic structure in adulthood.

Regarding the sleep-wake behavior, for the total time spent awake during the dark period, two-way ANOVA revealed a significant stress × drug interaction ($F_{1,17} = 27.44$, $P < 0.001$) and the main effect of stress ($F_{1,17} = 6.603$, $P = 0.020$; Fig. 3B). The interaction resulted from the finding that antalarmin treatment reversed the increase in stress-induced wakefulness ($P < 0.01$; Bonferroni's test). Similar reversal effects of antalarmin were found for the stress-induced decrease in NREM sleep during the dark period (Fig. 3D). For the REM sleep time,
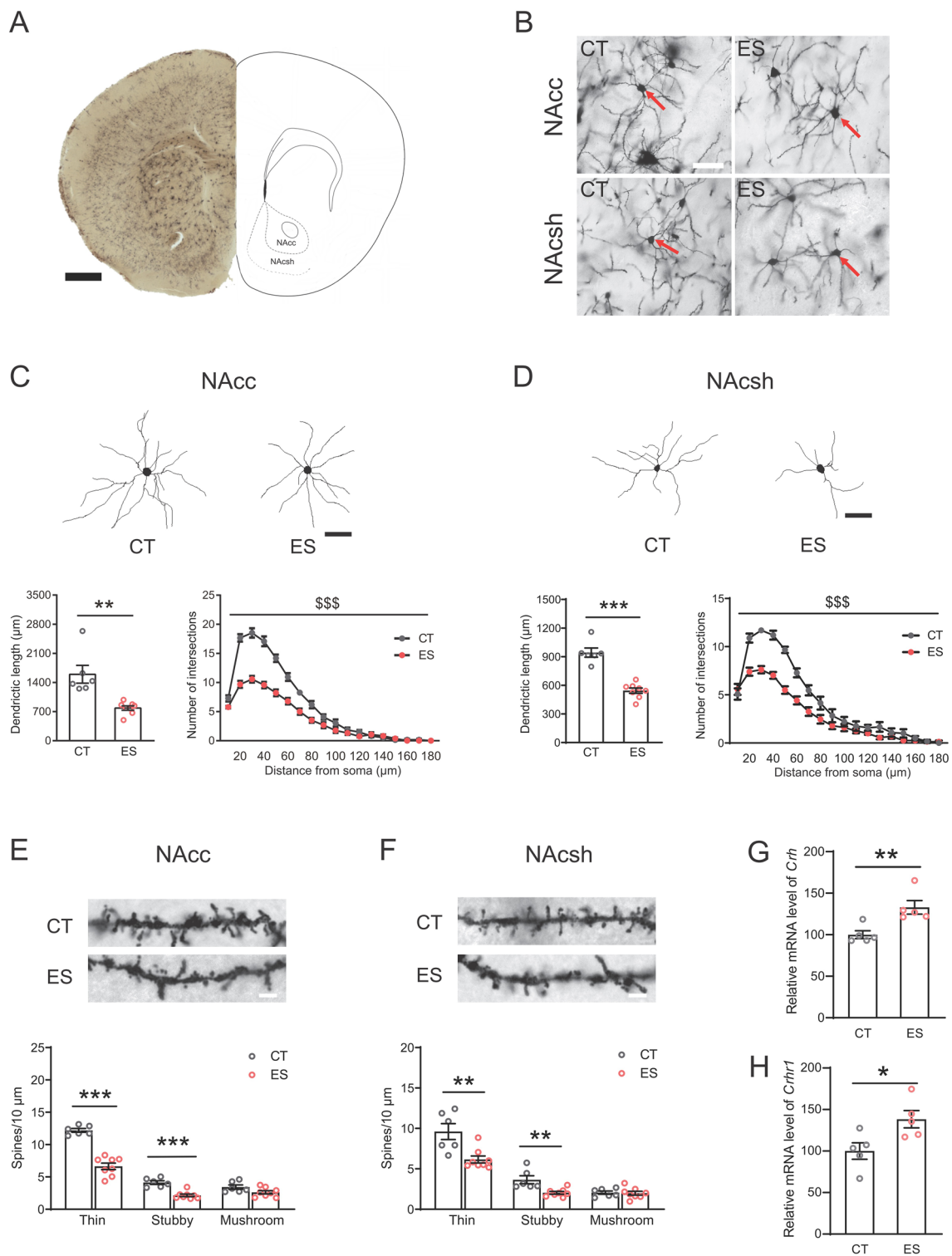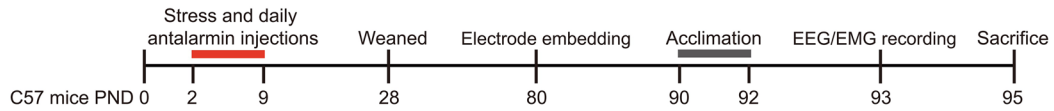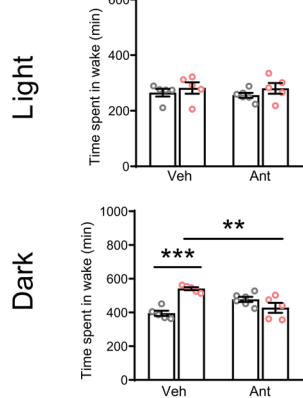
Fig. 2 Effects of early-life stress on the dendritic structure and spine density of NAc neurons. **A** Golgi-stained coronal section (scale bar, 500 μm) and a diagram of a coronal section showing two regions of interest [dashed area; NAc core (NAcc), NAc shell (NAcsh)]. **B** Representative images of Golgi-impregnated core and shell NAc neurons and respective tracings of dendrites, marked with the red arrows (scale bar, 50 μm). **C, D** Early-life stress reduces the length and com-plexity of dendrites in the NAcc (**C**) and NAcsh (**D**) (scale bars, 50 μm). **E, F** Early-life stress reduces spine density on dendrites in the NAcc (**E**) and NAcsh (**F**) (scale bars, 5 μm). CT, control; ES, early-life stress. *$P < 0.05$, **$P < 0.01$, ***$P < 0.001$, for group differences; independent-samples *t*-tests; CT: $n = 6$; ES: $n = 8$. $^{\$\$\$}P < 0.001$, for the main effect of stress; repeated measures ANOVA; CT: $n = 6$; ES: $n = 8$.
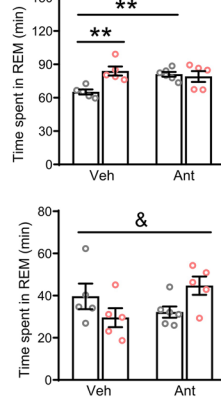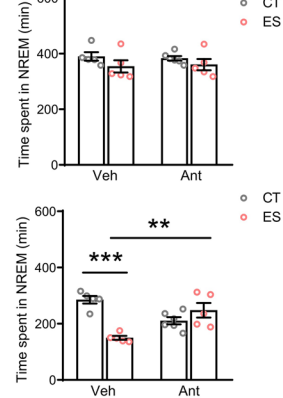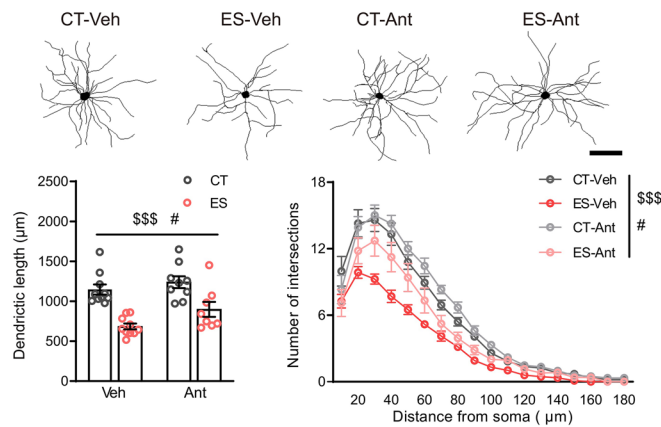
A Experimental design

B Wakefulness
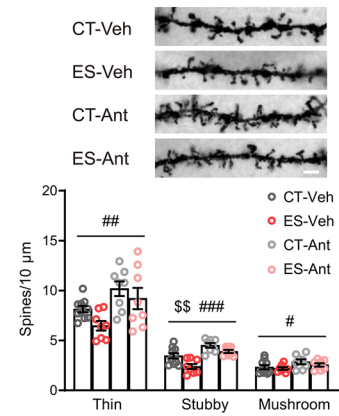## C REM sleep
D NREM sleep

Light

Dark

E NAcc

CT-Veh ES-Veh CT-Ant ES-Ant

F NAcc

CT-Veh
ES-Veh
CT-Ant
ES-Ant

G NAcsh

CT-Veh ES-Veh CT-Ant ES-Ant

H NAcsh

CT-Veh
ES-Veh
CT-Ant
ES-Ant

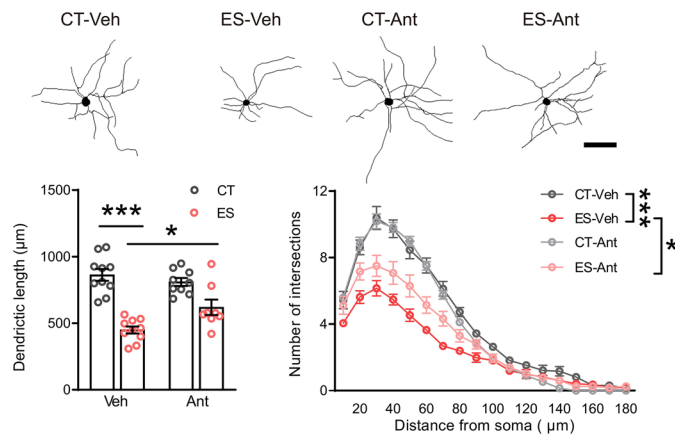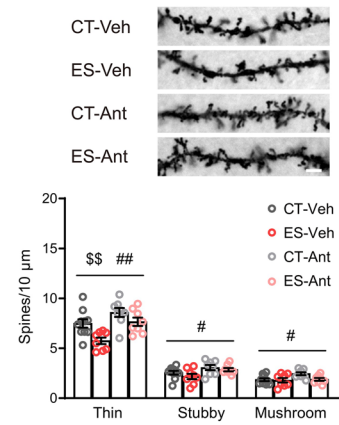◄**Fig. 3** Effects of CRHR1 blockade by antalarmin on early-life stress-induced sleep disturbance and NAc dendritic atrophy during adulthood. **A** Schematic of the design of Experiment 2. **B** Stress-induced increase of wakefulness time during the dark period is blocked by antalarmin. **C** For REM sleep, early-life stress significantly increases total REM time during the light period in vehicle-treated mice, whereas stressed mice show REM time comparable with control mice receiving antalarmin. Antalarmin also increases total REM time in the control mice. For the REM time during the dark period, there is a significant stress×drug interaction, yet group differences do not approach significance. **D** Stress-induced decrease of NREM time during the dark period is blocked by antalarmin. **E** CRHR1 blockade attenuates the lasting influence of early-life stress on dendritic complexity but not length, in the NAcc (scale bar, 50 μm). **F** Antalarmin increases the density of three spine types in the NAcc (scale bar, 5 μm). **G** CRHR1 blockade reverses the lasting influences of early-life stress on dendritic length and complexity in the NAcsh (scale bar, 50 μm). **H** Antalarmin increases the density of three spine types in the NAcsh (scale bar, 5 μm). Ant, antalarmin; CT, control; ES, early-life stress; NREM, non-rapid eye movement; PND, postnatal day; REM, rapid eye movement; Veh, vehicle. $*P<0.05$, $**P<0.01$, $***P<0.001$, for group differences; $^{\&}P<0.05$, for the stress×drug interaction; $^{\#}P<0.05$, $^{\#\#}P<0.01$, $^{\#\#\#}P<0.001$, for the main effect of drug; $^{\$\$}P<0.01$, $^{\$\$\$}P<0.001$, for the main effect of stress. Two-way ANOVA for sleep-wake test ($n=5$–6 per group), dendritic length ($n=8$–10 per group), and spine density ($n=8$–10 per group); repeated measures ANOVA for number of intersections ($n=8$–10 per group).

a significant stress×drug interaction was found during the light period ($F_{1,17}=9.195$, $P=0.008$; Fig. 3C, upper). Early-life stress increased the REM sleep time in the vehicle-treated mice ($P=0.009$; Bonferroni's test), which is consistent with previous studies [12–15], and did not significantly influence the REM sleep time in antalarmin-treated mice ($P>0.05$; Bonferroni's test). Furthermore, in control mice, antalarmin significantly increased the total REM sleep time ($P=0.022$; Bonferroni's test). Similar stress×drug interaction effects were found in the mean duration of REM sleep during the light period (Fig. S4). For the REM sleep time during the dark period, a significant stress×drug interaction was found ($F_{1,33}=6.595$, $P=0.020$; Fig. 3C, lower), yet group differences did not approach significance in the *post hoc* tests.

Regarding the NAc structural plasticity, antalarmin treatment attenuated the negative stress effects on dendritic length and complexity in the NAc shell (stress×drug interaction: length, $F_{1,33}=7.541$, $P=0.010$; complexity, $F_{1,33}=7.891$, $P=0.008$; Fig. 3G). For other morphological measures, the main effects of antalarmin treatment were an increased dendritic length ($F_{1,33}=5.142$, $P=0.030$) and complexity ($F_{1,33}=5.437$, $P=0.026$) in the NAc core (Fig. 3E) and in the densities of the three spine types across the two subregions (all $F_{1,30}>4.183$, all $P<0.05$; Fig. 3F, H). These results indicate that systemic antalarmin administration during stress exposure reverses early-life stress-induced dendritic simplification, but not spine loss, in the NAc.

CRH Overexpression in the NAc Reproduces Early-Life Stress-Induced Sleep Disturbance and NAc Dendritic Atrophy
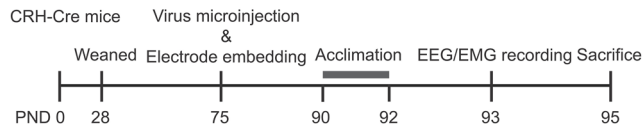
To test the possibility that the CRH–CRHR1 system in the NAc mediates early-life stress-induced sleep disturbances, we first determined whether overexpressing CRH in the NAc (mimicking the effects of stress) could reproduce the stress effects on sleep-wake behavior and NAc dendritic morphology. CRH overexpression was achieved by bilateral stereotaxic injections of a Cre-recombinase-dependent AAV vector carrying the *Crh* sequence (AAV-CAG-DIO-CRH-P2A-GFP) into the NAc of CRH-Cre mice (PND75; Fig. 4A, B). Two weeks after the AAV injection, CRH expression ($t_8=3.293$, $P=0.011$, Fig. 4C) and *Crh* mRNA levels ($t_5=2.980$, $P=0.031$, Fig. 4D) in the NAc of mice receiving target virus were significantly higher than those of mice receiving control virus.

During the dark period, similar to the effects of early-life stress, CRH overexpression in the NAc significantly increased the time spent awake ($t_{10}=2.689$, $P=0.023$, Fig. 4E). CRH overexpression also reduced the REM sleep time ($t_{10}=2.284$, $P=0.046$, Fig. 4F right), which was associated with a decreased number of REM episodes ($t_{10}=2.415$, $P=0.036$, Fig. S5B right), and the NREM sleep time ($t_{10}=2.653$, $P=0.024$, Fig. 4G), which was associated with decreased mean duration of NREM sleep per episode ($t_{10}=2.529$, $P=0.030$, Fig. S5A). During the light period, CRH overexpression in the NAc increased REM sleep time ($t_{10}=3.771$, $P=0.004$, Fig. 4F left), which was associated with an increased number of REM episodes during the light period ($t_{10}=2.389$, $P=0.038$, Fig. S5B left).
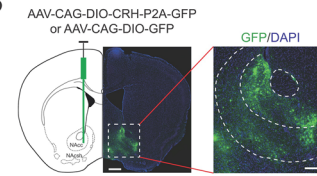
Regarding the NAc dendritic morphology, compared with control mice, CRH overexpression in the NAc significantly reduced the length (NAcc: $t_{10}=7.839$, $P<0.001$; NAcsh: $t_{10}=4.854$, $P<0.001$) and complexity (NAcc: $F_{1,10}=43.59$, $P<0.001$; NAcsh: $F_{1,10}=20.05$, $P<0.001$) of dendrites in both NAcc (Fig. 4H) and NAcsh (Fig. 4J). In line with the effects of early-life stress, spine loss was observed in mice with CRH overexpression on thin (NAcc: $t_{10}=9.289$, $P<0.001$; NAcsh: $t_{10}=9.730$, $P<0.001$) and stubby (NAcc: $t_{10}=3.359$, $P=0.010$; NAcsh: $t_{10}=2.549$, $P=0.03$) spines in both NAcc (Fig. 4I) and NAcsh (Fig. 4K). The area of the cell body was not significantly affected by CRH overexpression in either NAcc (Fig. S6A) or NAcsh (Fig. S6B).

These results indicate that NAc CRH overexpression largely reproduces the effects of early-life stress on sleep-wake behavior and NAc dendritic morphology.
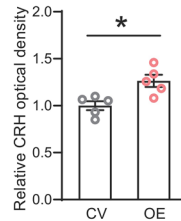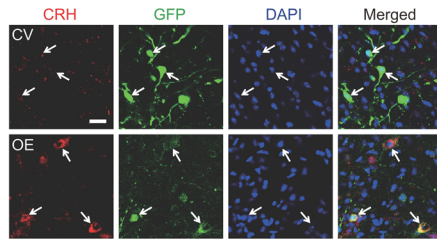
A Experimental design

CRH-Cre mice | Virus microinjection & Electrode embedding | Acclimation | EEG/EMG recording Sacrifice

Weaned

PND 0 | 28 | 75 | 90 | 92 | 93 | 95

B AAV-CAG-DIO-CRH-P2A-GFP or AAV-CAG-DIO-GFP

GFP/DAPI

C CRH | GFP | DAPI | Merged

CV

OE

Relative CRH optical density

D Relative mRNA level of *Crh*

E Wakefulness

F REM sleep

G NREM sleep

H NAcc

I NAcc

J NAcsh

K NAcsh
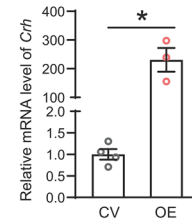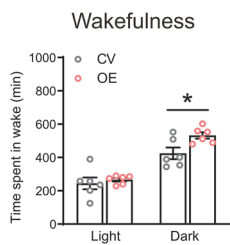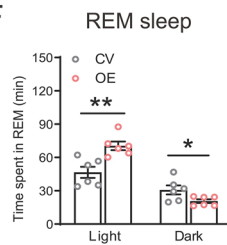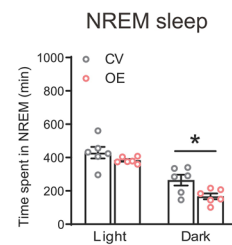
◄**Fig. 4** Effects of NAc CRH overexpression on sleep-wake behavior and NAc dendritic morphology. **A** Schematic of the design of Experiment 3. **B** Left panel, schematic of AAV microinjection into the NAc of adult CRH-Cre mice; right panel, region-specific expression of GFP in the NAc (scale bars, 500 μm and 200 μm). **C** Representative images showing the expression of CRH, GFP, and DAPI in the NAc of control and CRH-OE mice (independent-samples *t*-tests; CV: $n=5$; OE: $n=5$). Arrowheads indicate EGFP-expressing neurons (scale bar, 20 μm). **D** 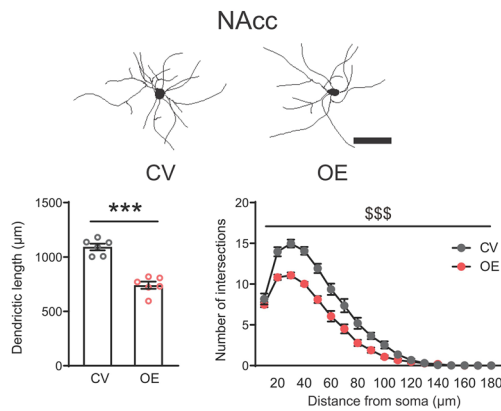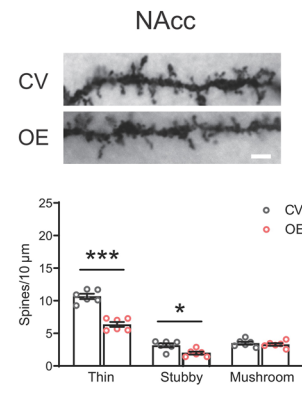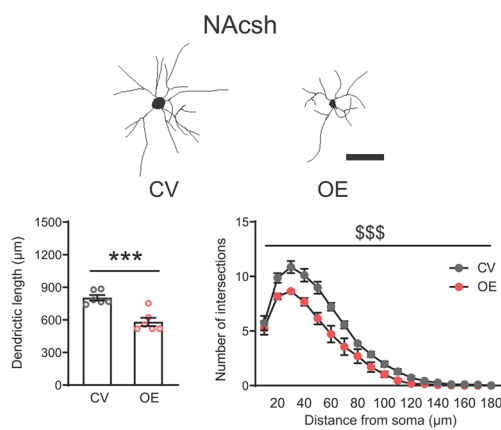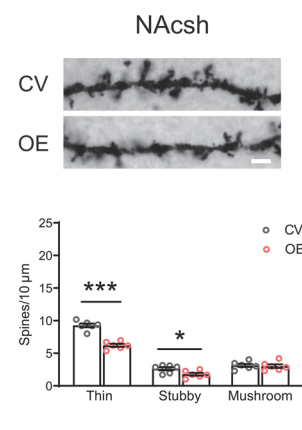RT-PCR analyses confirm the overexpression-induced increase of *Crh* mRNA levels in the NAc (independent-samples *t*-tests; CV: $n=4$; OE: $n=3$). **E** NAc CRH overexpression increases wakefulness during the dark period (independent-samples *t*-tests; CV: $n=6$; OE: $n=6$). **F** NAc CRH overexpression increases REM sleep time during the light period and decreases REM sleep time during the dark period (independent-samples *t*-tests; CV: $n=6$; OE: $n=6$). **G** NAc CRH overexpression decreases NREM sleep time during the dark period (independent-samples *t*-tests; CV: $n=6$; OE: $n=6$). **H, J** NAc CRH overexpression reduces the length (independent-samples *t*-tests; CV: $n=6$; OE: $n=6$) and complexity of dendrites (repeated measures ANOVA; CV: $n=6$; OE: $n=6$) in both the NAcc (**H**) and NAcsh (**J**) (scale bar, 50 μm). **I, K** CRH overexpression reduces spine density (independent-samples *t*-tests; CV: $n=6$; OE: $n=6$) in both the NAcc (**I**) and NAcsh (**K**) (scale bar, 5 μm). CV, control virus; NREM, non-rapid eye movement; OE, NAc CRH overexpression; PND, postnatal day; REM, rapid eye movement. *$*P<0.05$, $**P<0.01$, $***P<0.001$, for group differences; $^{\$\$\$}P<0.001$, for the main effect of virus.

CRHR1 Knockdown in the NAc Reverses Early-Life Stress-Induced Sleep Disturbance and NAc Dendrite Atrophy

Finally, we investigated whether NAc CRHR1 knockdown (Fig. 5A) could reverse the negative effects of early-life stress. CRHR1 knockdown was achieved by injecting the pLent-U6-shCRHR1-GFP virus into the NAc (Fig. 5B). *Crhr1* mRNA levels ($t_9=3.076$, $P=0.013$; Fig. 5B) and CRHR1 expression ($t_{16}=2.366$, $P=0.031$; Fig. 5C) were significantly reduced in the NAc following CRHR1 knockdown.

Regarding the sleep-wake behavior, for the total time spent awake during the dark period (Fig. 5D, upper), two-way ANOVA revealed a significant main effect of stress ($F_{1,20}=7.156$, $P=0.015$) and a stress × virus interaction ($F_{1,20}=5.452$, $P=0.030$) in that the increased wakefulness in stressed mice was partially reversed by CRHR1 knockdown in the NAc (Fig. 5D, upper). Similar reversal effects of NAc CRHR1 knockdown were found for the NREM sleep time (Fig. 5D, lower). REM sleep time during the light period (Fig. 5D, middle) showed a significant main effect of stress ($F_{1,20}=7.229$, $P=0.014$), without a stress × virus interaction ($P>0.05$), indicating that the increase in REM sleep induced by stress was not reversed by CRHR1 knockdown in the NAc. Interestingly, NAc CRHR1 knockdown reversed the stress-induced increase in the mean duration of REM sleep, as supported by the significant stress × virus interaction ($F_{1,20}=8.037$, $P=0.010$; Fig. S7).

Regarding the NAc dendritic morphology, significant stress × virus interactions were found for dendritic length and complexity in both the NAcc (length: $F_{1,20}=64.69$, $P<0.001$; complexity: $F_{1,20}=24.22$, $P<0.001$; Fig. 5E) and the NAcsh (length: $F_{1,20}=232.2$, $P<0.001$; complexity: $F_{1,20}=27.46$, $P<0.001$; Fig. 5G). Group comparisons showed that the dendritic simplification induced by early-life stress was reversed by NAc CRHR1 knockdown (Fig. 5E, G). NAc CRHR1 knockdown also normalized the stress-induced loss of thin and stubby spines in the NAcc (stress × virus interaction, thin: $F_{1,20}=6.247$, $P=0.021$; stubby: $F_{1,20}=7.078$, $P=0.015$; Fig. 5F), but not in the NAcsh (Fig. 5H).
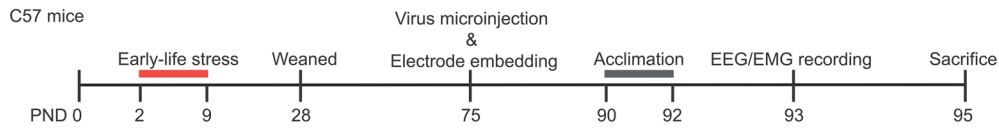
These results indicated that NAc CRHR1 knockdown successfully reversed the early-life stress-induced abnormalities in sleep-wake behavior (including increased wakefulness and reduced NREM sleep during the dark period) and NAc dendritic structure in adulthood.
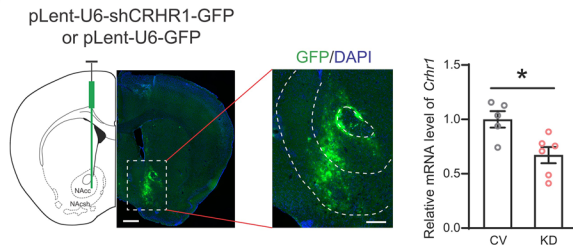
Discussion

In this study, we determined whether the CRH–CRHR1 system in the NAc mediates early-life stress-induced abnormalities in sleep-wake behavior. We first demonstrated that exposure to early-life stress leads to sleep disturbances, including increased wakefulness and reduced NREM sleep in the dark period and increased REM sleep in the light period, which were accompanied by a simplified dendritic structure, spine loss, and elevated CRH–CRHR1 signaling in the NAc. The negative effects of early-life stress on sleep behaviors and NAc dendritic structure were largely normalized by concurrent CRHR1 blockade. More importantly, we found that CRH overexpression in the NAc reproduced the effects of early-life stress, while NAc CRHR1 knockdown reversed many of the negative effects of early-life stress (including increased wakefulness and reduced NREM sleep in the dark period and NAc dendritic atrophy). Together, our findings highlight the CRH–CRHR1 system in the NAc as a key mediator of the early-life stress-induced sleep disturbances during adulthood (Fig. 6).

Using various early-life stress paradigms (maternal separation, cross-fostering, and prenatal stress), several groups have reported that rodents exposed to early-life stress show more REM sleep than controls during the light period [12–15]. We have largely replicated this result in the early-life stress paradigm of the nesting and bedding material procedure (especially in Experiments 2 and 4), providing evidence that increased REM sleep in adulthood is a relatively universal outcome of stressful early-life experiences. Importantly, regarding the sleep-wake behavior during the dark period, previous studies either did not collect the data due to their primary focus on the inactive (light) period

A Experimental design

C57 mice

Early-life stress | Weaned | Virus microinjection & Electrode embedding | Acclimation | EEG/EMG recording | Sacrifice

PND 0 — 2 — 9 — 28 — 75 — 90 — 92 — 93 — 95

B pLent-U6-shCRHR1-GFP or pLent-U6-GFP

GFP/DAPI

Relative mRNA level of *Crhr1*

CV | KD

C

CRHR1 | GFP | DAPI | Merged

CV

KD

Relative CRHR1 optical density

CT | KD

D

Light | Dark

Wakefulness — Time spent in wake (min) — CT, ES — CV, KD — *P* = 0.02

REM sleep — Time spent in REM (min) — $ — CV, KD

NREM sleep — Time spent in NREM (min) — *P* = 0.025

E NAcc

CT-CV | ES-CV | CT-KD | ES-KD

Dendritic length (μm) — CT, ES — CV, KD

Number of intersections — CT-CV, ES-CV, CT-KD, ES-KD — Distance from soma (μm)

F NAcc

CT-CV | ES-CV | CT-KD | ES-KD

Spines/10 μm — CT-CV, ES-CV, CT-KD, ES-KD — Thin, Stubby, Mushroom — *P* = 0.018, *P* = 0.019, $$

G NAcsh

CT-CV | ES-CV | CT-KD | ES-KD

Dendritic length (μm) — CT, ES — CV, KD

Number of intersections — CT-CV, ES-CV, CT-KD, ES-KD — Distance from soma (μm)

H NAcsh

CT-CV | ES-CV | CT-KD | ES-KD

Spines/10 μm — CT-CV, ES-CV, CT-KD, ES-KD — Thin, Stubby, Mushroom — #

◀**Fig. 5** Effects of NAc CRHR1 knockdown on early-life stress-induced sleep disturbance and NAc dendritic atrophy during adulthood. **A** Schematic of the design of Experiment 4. **B** Left panel, schematic of AAV microinjection into the NAc of adult C57BL/6N mice; middle panel, region-specific expression of GFP in the NAc (scale bars, 500 μm and 200 μm); right panel, RT-PCR analyses confirm the knockdown-induced reduction of *Crhr1* mRNA levels in the NAc (independent-samples *t*-tests; CV: $n=5$; KD: $n=6$). **C** Representative images showing the expression of CRHR1, GFP, and DAPI in the NAc of control and CRHR1-KD mice (independent-samples *t*-tests; CV: $n=8$; KD: $n=10$). Arrowheads indicate EGFP-expressing neurons, and asterisks indicate uninfected neurons (scale bar, 40 μm). **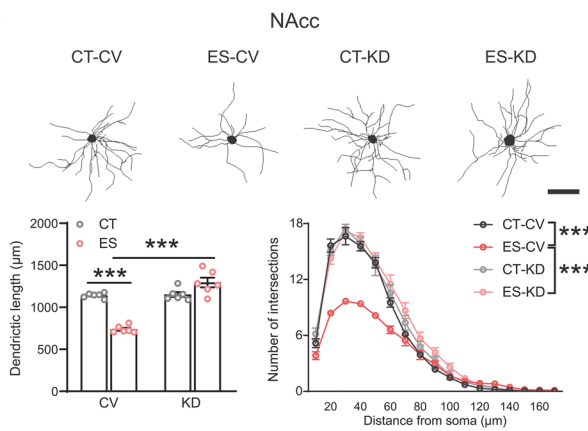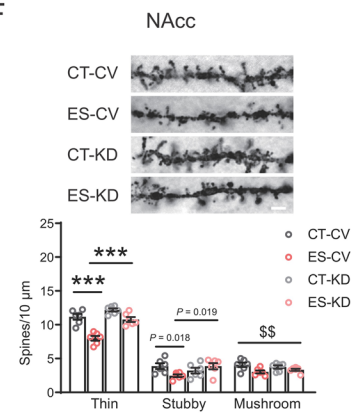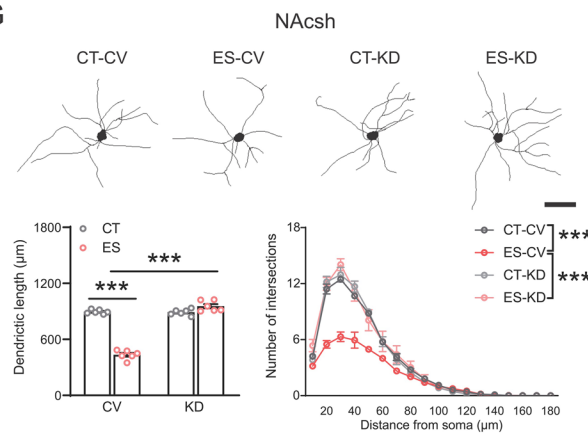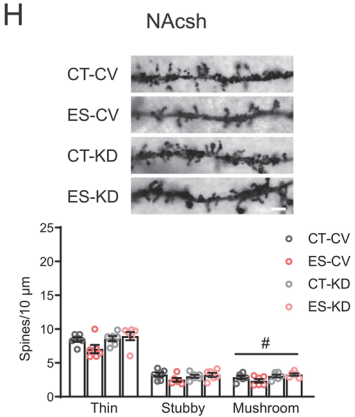D** Effects of NAc CRHR1 knockdown on early-life stress-induced sleep disturbance. Upper panel, CRHR1 knockdown normalizes the stress-induced increase of wakefulness during the dark period. Middle panel, early-life stress increases REM sleep during the light period, which is not reversed by NAc CRHR1 knockdown. Lower panel, CRHR1 knockdown normalizes stress-induced reduction of NREM time during the dark period (two-way ANOVA; $n=6$ per group). **E, G** NAc CRHR1 knockdown normalizes the dendritic arborization (length: two-way ANOVA; $n=6$ per group; complexity: repeated measures ANOVA; $n=6$ per group) of NAcc and NAcsh neurons in mice exposed to early-life stress (scale bar, 50 μm). **F** NAc CRHR1 knockdown normalizes the thin and stubby spine density in the NAcc (two-way ANOVA; $n=6$ per group). **H** CRHR1 knockdown increases mushroom spine density in the NAcsh (two-way ANOVA; $n=6$ per group). CT, control; CV, control virus; ES, early-life stress; KD, CRHR1 knockdown; NREM, non-rapid eye movement; PND, postnatal day; REM, rapid eye movement. $*P<0.05$, $***P<0.001$, for group differences surviving Bonferroni correction; $^{\$\$}P<0.01$, for the main effect of stress; $^{\#}P<0.05$, for the main effect of virus.

or did not find any stress effects in rats [12–15]. Here, we found that early-life stress increased total wakefulness and decreased NREM sleep during the dark period. This discrepancy could arise from differences in strain (rats or mice) or stress paradigms [10, 43]. Despite the fact that mice are more active during the dark period, they still sleep for about a third of the time (based on our observations). The disruption of this sleep-wake pattern by early-life stress may have functional implications that await future investigation; the stress-induced increase in REM sleep during the light period may compensate for this disruption.

CRH is a central neuropeptide in the adaptation to stress and plays a key role in the regulation of sleep and the maintenance of wakefulness [21]. ICV or intraventricular administration of CRH has been shown to increase REM sleep and wakefulness and to decrease the amount of slow-wave sleep (also known as NREM) in humans and rodents [23, 24, 44]. CRHR1 receptor antagonists have been considered as promising candidates to treat sleep changes in depression [45–47]. For example, a four-week treatment with a CRH antagonist (R121919) decreased REM density and the number of awakenings and increased slow-wave sleep in patients with depression [20]. In our study, we found that systemic CRHR1 blockade (*via* antalarmin treatment) during stress exposure abolished the negative effects of early-life stress on wakefulness and NREM sleep, providing evidence for

the involvement of the CRH–CRHR1 system in early-life stress-induced sleep alterations. Interestingly, while interaction between antalarmin and stress was found for REM sleep, since antalarmin increased REM sleep during the light period in the control mice, we cannot simply conclude that antalarmin reverses the effects of stress on REM sleep. Previously, it has been shown that CRHR1 knockout abolishes the effects of ICV injections of CRH on wakefulness and NREM sleep, but not REM sleep [24]. Together, these results suggest that systemic or regionally-nonspecific CRH–CRHR1 manipulation has a rather complex impact on REM sleep.

The CRH–CRHR1 system in different brain regions may play different roles in sleep regulation. For instance, it has been found that CRH overexpression in either the entire brain or in the forebrain in transgenic mice increases REM sleep during the light period, whereas alterations of NREM sleep are only induced by CRH overexpression throughout the brain, not by CRH overexpression in the forebrain [22]. Our study for the first time showed that CRH overexpression in the NAc by virus injection altered the sleep-wake behavior, such as increased REM during the light period, and increased wakefulness and decreased NREM sleep during the dark period. Previous studies have shown that the NAc regulates sleep by the activity of D1-MSNs or D2-MSNs [36, 48, 49], which express CRHR1 [30, 50]. It is thus possible that these MSNs mediate the effects of NAc CRH overexpression on sleep we observed. Importantly, the sleep alterations induced by NAc CRH overexpression were largely similar to those of early-life stress. Together with the finding that early-life stress up-regulated CRH mRNA levels in the NAc, these findings lend support to the potential involvement of NAc CRH-expressing neurons in the negative effects of early-life stress. Furthermore, NAc CRHR1 knockdown prevented the stress-induced alterations (increased wakefulness and decreased NREM sleep during the dark period, increased mean duration of REM sleep during the light period), indicating that the NAc CRH–CRHR1 system contributes to the negative effects of early-life stress on sleep-wake behavior. As robust CRH-expressing afferents to the NAc originate in the paraventricular nucleus of the thalamus, the bed nucleus of the stria terminalis, the medial prefrontal cortex, and the basolateral amygdala [51], it should be noted that our findings so far could not disentangle whether the negative influences of early-life stress are mediated by NAc CRH neurons, NAc CRH afferents, or both. Future studies are encouraged to specifically manipulate CRH expression in CRH-positive neurons in either the NAc or regions projecting to NAc.

The abnormal morphological changes of NAc neurons may constitute the structural basis of sleep disturbances caused by early-life stress. Only a few studies have examined the effects of early-life stress on the structural plasticity of
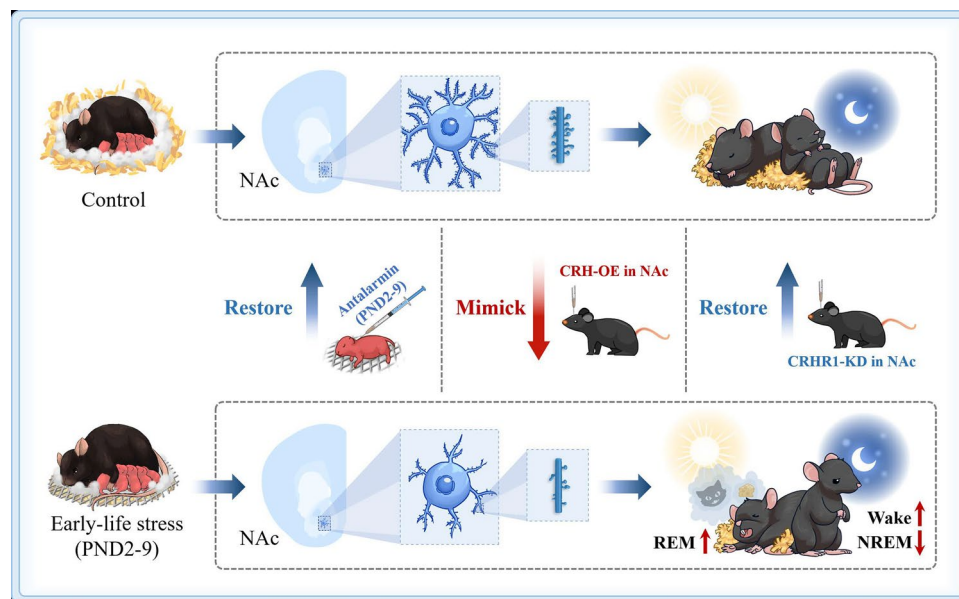
Fig. 6 Summary of the role of the NAc CRH–CRHR1 system in early-life stress-induced sleep disturbance and dendritic atrophy in adulthood. Early-life stress lastingly increases the CRH–CRHR1 signaling and destroys the morphological plasticity in the NAc, including simplified dendritic structure and spine loss, which in turn leads to sleep disturbances, including increased REM sleep in the light period and increased wakefulness and reduced NREM sleep in the dark period. Concurrent CRHR1 blockade by antalarmin during stress exposure normalizes the negative effects of early-life stress on the NAc and reported inconsistent results. While increases the NAc dendritic structure. CRH overexpression in the NAc reproduces the effects of early-life stress, while NAc CRHR1 knockdown reverses the negative effects of early-life stress. These findings highlight the CRH–CRHR1 system in the NAc as a key mediator of early-life stress-induced sleep disturbances during adulthood. CRH, corticotropin-releasing hormone; CRHR1, corticotropin-releasing hormone receptor 1; KD, knockdown; NAc, nucleus accumbens; NREM, non-rapid eye movement; OE, overexpression; PND, postnatal day; REM, rapid eye movement.

the NAc and reported inconsistent results. While increases in dendritic branching and length and/or spine density in the NAc during adulthood have been found following prenatal elevated Plexiglas platform stress (gestation from days 11–16) or maternal separation (PND3–21, 3 h per day) [52], spine loss (without changes in dendritic length) has been found following long-term restraint stress during pregnancy (gestation from day 11 to delivery, 2 h per day) [53]. Here we found more devastating effects of the limited nesting and bedding material paradigm on dendritic structure in adulthood (including dendritic simplification and spine loss). We further found that NAc CRHR1 knockdown normalized the stress-induced dendritic simplification in the NAc, providing evidence for the involvement of the CRH-CRHR1 system in the integrity of the dendritic structure. Regarding the effects of antalarmin treatment, while our previous work in the hippocampus and frontal cortex showed that antalarmin largely reverses stress-induced dendritic atrophy [19, 33], here we found that antalarmin partially reversed stress-induced dendritic simplification and increased the spine density in the NAc, suggesting regional specificity of early antalarmin prevention. In addition, while the core and shell of NAc may play different roles in sleep regulation [49], we did not find subregion specificity, as the dendritic structure in both subregions was vulnerable to early-life

stress and was restored by CRHR1 blockade, which indicates that the CRH–CRHR1 system in both subregions may be similarly involved in early-life stress-induced sleep disturbances. Besides morphological deficits, we also found that early-life stress reduced the VGluT1/VGAT ratio in the NAc. Together with our similar report in aged mice [29], these results indicate that early-life stress-induced sleep alterations are accompanied by excitatory-inhibitory imbalance in the NAc.

The study has several limitations. First, we found variations in sleep-wake behavioral indices across experiments in control mice, especially in the amount of REM time. Possible reasons for these variations include different animal cohorts or subjective coding schemes; future studies are encouraged to apply automatic analysis pipelines to avoid coding subjectivity. Nevertheless, our conclusions are not undermined by the variations in baseline values across experiments, as our results were based on group differences in the same cohort and the experimenter was blind to experimental treatments. Second, while NAc CRHR1 knockdown during adulthood largely reversed early-life stress-induced sleep-wake abnormalities, it remains unclear whether there is a critical time window for the treatment or intervention of early-life stress on sleep-wake behaviors. It should be noted that NAc CRHR1 knockdown did not restore REM

sleep during the light period (except for the mean duration of REM sleep). In addition, one recent study reported that early-life stress in rats induces a lifelong decrease in sleep spindles (in weaning, early adult, and older adult) [54]. These findings call for early treatment or intervention. Indeed, previous studies have demonstrated the efficacy of early intervention, showing that early-life stress-induced deficits in hippocampal dendritic morphology are effectively reversed by CRHR1 blockade immediately after stress exposure (PND10–17) [55] or prolonged CRHR1 blockade (PND2–14) [33]. Future studies are warranted to examine the effects of early-life stress on sleep-wake behaviors in younger mice and to compare treatment efficacy across several age periods to identify the critical time window for intervention.

In summary, this study reveals a critical role of the NAc CRH–CRHR1 system in mediating early-life stress-induced sleep disturbances (including increased wakefulness and reduced NREM sleep during the dark period). While the translation of these findings to clinical situations is currently premature, the development of CRHR1-based or NAc-targeted therapeutic strategies may open up new avenues for the treatment of stress-induced sleep disturbances.

Conflict of interest The authors claim that there are no conflict of interest.

References

1. LeMoult J, Humphreys KL, Tracy A, Hoffmeister JA, Ip E, Gotlib IH. Meta-analysis: Exposure to early life stress and risk for depression in childhood and adolescence. J Am Acad Child Adolesc Psychiatry 2020, 59: 842–855.

2. Lippard ETC, Nemeroff CB. The devastating clinical consequences of child abuse and neglect: Increased disease vulnerability and poor treatment response in mood disorders. Am J Psychiatry 2020, 177: 20–36.

3. Short AK, Baram TZ. Early-life adversity and neurological disease: Age-old questions and novel answers. Nat Rev Neurol 2019, 15: 657–669.

4. Bader K, Schäfer V, Schenkel M, Nissen L, Schwander J. Adverse childhood experiences associated with sleep in primary insomnia. J Sleep Res 2007, 16: 285–296.

5. Chapman DP, Wheaton AG, Anda RF, Croft JB, Edwards VJ, Liu Y. Adverse childhood experiences and sleep disturbances in adults. Sleep Med 2011, 12: 773–779.

6. Greenfield EA, Lee C, Friedman EL, Springer KW. Childhood abuse as a risk factor for sleep problems in adulthood: Evidence from a US national study. Ann Behav Med 2011, 42: 245–256.

7. Gregory AM, Caspi A, Moffitt TE, Poulton R. Family conflict in childhood: A predictor of later insomnia. Sleep 2006, 29: 1063–1067.

8. Koskenvuo K, Hublin C, Partinen M, Paunio T, Koskenvuo M. Childhood adversities and quality of sleep in adulthood: A population-based study of 26, 000 Finns. Sleep Med 2010, 11: 17–22.

9. Palagini L, Drake CL, Gehrman P, Meerlo P, Riemann D. Early-life origin of adult insomnia: Does prenatal-early-life stress play a role? Sleep Med 2015, 16: 446–456.

10. Lo Martire V, Caruso D, Palagini L, Zoccoli G, Bastianini S. Stress & sleep: A relationship lasting a lifetime. Neurosci Biobehav Rev 2020, 117: 65–77.

11. Dugovic C, Maccari S, Weibel L, Turek FW, van Reeth O. High corticosterone levels in prenatally stressed rats predict persistent paradoxical sleep alterations. J Neurosci 1999, 19: 8656–8664.

12. Mrdalj J, Pallesen S, Milde AM, Jellestad FK, Murison R, Ursin R, *et al.* Early and later life stress alter brain activity and sleep in rats. PLoS One 2013, 8: e69923.

13. Sampath D, Sabitha KR, Hegde P, Jayakrishnan HR, Kutty BM, Chattarji S, *et al.* A study on fear memory retrieval and REM sleep in maternal separation and isolation stressed rats. Behav Brain Res 2014, 273: 144–154.

14. Santangeli O, Lehtikuja H, Palomäki E, Wigren HK, Paunio T, Porkka-Heiskanen T. Sleep and behavior in cross-fostering rats: Developmental and sex aspects. Sleep 2016, 39: 2211–2221.

15. Tiba PA, Tufik S, Suchecki D. Effects of maternal separation on baseline sleep and cold stress-induced sleep rebound in adult Wistar rats. Sleep 2004, 27: 1146–1153.

16. Li JT, Xie XM, Yu JY, Sun YX, Liao XM, Wang XX, *et al.* Suppressed calbindin levels in hippocampal excitatory neurons mediate stress-induced memory loss. Cell Rep 2017, 21: 891–900.

17. Wang C, Liu H, Li K, Wu ZZ, Wu C, Yu JY, *et al.* Tactile modulation of memory and anxiety requires dentate granule cells along the dorsoventral axis. Nat Commun 2020, 11: 6045.

18. Rice CJ, Sandman CA, Lenjavi MR, Baram TZ. A novel mouse model for acute and long-lasting consequences of early life stress. Endocrinology 2008, 149: 4892–4900.

19. Yang XD, Liao XM, Uribe-Mariño A, Liu R, Xie XM, Jia J, *et al.* Stress during a critical postnatal period induces region-specific structural abnormalities and dysfunction of the prefrontal cortex *via* CRF1. Neuropsychopharmacology 2015, 40: 1203–1215.

20. Held K, Künzel H, Ising M, Schmid DA, Zobel A, Murck H, *et al.* Treatment with the CRH1-receptor-antagonist R121919 improves sleep-EEG in patients with depression. J Psychiatr Res 2004, 38: 129–136.

21. Steiger A, Dresler M, Kluge M, Schüssler P. Pathology of sleep, hormones and depression. Pharmacopsychiatry 2013, 46: S30–S35.

22. Kimura M, Müller-Preuss P, Lu A, Wiesner E, Flachskamm C, Wurst W, *et al.* Conditional corticotropin-releasing hormone over-expression in the mouse forebrain enhances rapid eye movement sleep. Mol Psychiatry 2010, 15: 154–165.

23. Chang FC, Opp MR. Blockade of corticotropin-releasing hormone receptors reduces spontaneous waking in the rat. Am J Physiol 1998, 275: R793–R802.

24. Romanowski CPN, Fenzl T, Flachskamm C, Wurst W, Holsboer F, Deussing JM, *et al.* Central deficiency of corticotropin-releasing hormone receptor type 1 (CRH-R1) abolishes effects of CRH on NREM but not on REM sleep in mice. Sleep 2010, 33: 427–436.

25. Bayassi-Jakowicka M, Lietzau G, Czuba E, Steliga A, Waśkow M, Kowiański P. Neuroplasticity and multilevel system of connections determine the integrative role of nucleus accumbens in the brain reward system. Int J Mol Sci 2021, 22: 9806.

26. Lazarus M, Chen JF, Urade Y, Huang ZL. Role of the basal ganglia in the control of sleep and wakefulness. Curr Opin Neurobiol 2013, 23: 780–785.

27. Lazarus M, Huang ZL, Lu J, Urade Y, Chen JF. How do the basal ganglia regulate sleep-wake behavior? Trends Neurosci 2012, 35: 723–732.

28. Qiu MH, Vetrivelan R, Fuller PM, Lu J. Basal ganglia control of sleep-wake behavior and cortical activation. Eur J Neurosci 2010, 31: 499–507.

29. Wang T, Wang HL, Liu R, Wang H, Zhang Y, Sun YX, *et al*. Early-life stress alters sleep structure and the excitatory-inhibitory balance in the nucleus accumbens in aged mice. Chin Med J (Engl) 2019, 132: 1582–1590.

30. Lemos JC, Wanat MJ, Smith JS, Reyes BAS, Hollon NG, van Bockstaele EJ, *et al*. Severe stress switches CRF action in the nucleus accumbens from appetitive to aversive. Nature 2012, 490: 402–406.

31. Kono J, Konno K, Talukder AH, Fuse T, Abe M, Uchida K, *et al*. Distribution of corticotropin-releasing factor neurons in the mouse brain: A study using corticotropin-releasing factor-modified yellow fluorescent protein knock-in mouse. Brain Struct Funct 2017, 222: 1705–1732.

32. Molet J, Maras PM, Avishai-Eliner S, Baram TZ. Naturalistic rodent models of chronic early-life stress. Dev Psychobiol 2014, 56: 1675–1688.

33. Liu R, Yang XD, Liao XM, Xie XM, Su YN, Li JT, *et al*. Early postnatal stress suppresses the developmental trajectory of hippocampal pyramidal neurons: The role of CRHR1. Brain Struct Funct 2016, 221: 4525–4536.

34. Naninck EFG, Hoeijmakers L, Kakava-Georgiadou N, Meesters A, Lazic SE, Lucassen PJ, *et al*. Chronic early life stress alters developmental and adult neurogenesis and impairs cognitive function in mice. Hippocampus 2015, 25: 309–328.

35. Liao XM, Yang XD, Jia J, Li JT, Xie XM, Su YN, *et al*. Blockade of corticotropin-releasing hormone receptor 1 attenuates early-life stress-induced synaptic abnormalities in the neonatal hippocampus. Hippocampus 2014, 24: 528–540.

36. Luo YJ, Li YD, Wang L, Yang SR, Yuan XS, Wang J, *et al*. Nucleus accumbens controls wakefulness by a subpopulation of neurons expressing dopamine D1 receptors. Nat Commun 2018, 9: 1576.

37. Glaser EM, van der Loos H. Analysis of thick brain sections by obverse-reverse computer microscopy: Application of a new, high clarity Golgi-Nissl stain. J Neurosci Methods 1981, 4: 117–125.

38. Sholl DA. Dendritic organization in the neurons of the visual and motor cortices of the cat. J Anat 1953, 87: 387–406.

39. Bourne JN, Harris KM. Balancing structure and function at hippocampal dendritic spines. Annu Rev Neurosci 2008, 31: 47–67.

40. Eiden LE. The vesicular neurotransmitter transporters: Current perspectives and future prospects. FASEB J 2000, 14: 2396–2400.

41. Wilson NR, Kang JS, Hueske EV, Leung T, Varoqui H, Murnick JG, *et al*. Presynaptic regulation of quantal size by the vesicular glutamate transporter VGLUT1. J Neurosci 2005, 25: 6221–6234.

42. Wojcik SM, Rhee JS, Herzog E, Sigler A, Jahn R, Takamori S, *et al*. An essential role for vesicular glutamate transporter 1 (VGLUT1) in postnatal development and control of quantal size. Proc Natl Acad Sci U S A 2004, 101: 7158–7163.

43. Pawlyk AC, Morrison AR, Ross RJ, Brennan FX. Stress-induced changes in sleep in rodents: Models and mechanisms. Neurosci Biobehav Rev 2008, 32: 99–117.

44. Holsboer F, von Bardeleben U, Steiger A. Effects of intravenous corticotropin-releasing hormone upon sleep-related growth hormone surge and sleep EEG in man. Neuroendocrinology 1988, 48: 32–38.

45. Griebel G, Holsboer F. Neuropeptide receptor ligands as drugs for psychiatric diseases: The end of the beginning? Nat Rev Drug Discov 2012, 11: 462–478.

46. Holsboer F, Ising M. Central CRH system in depression and anxiety—evidence from clinical studies with CRH1 receptor antagonists. Eur J Pharmacol 2008, 583: 350–357.

47. Holsboer F, Ising M. Stress hormone regulation: Biological role and translation into therapy. Annu Rev Psychol 2010, 61(81–109): C1-11.

48. McCullough KM, Missig G, Robble MA, Foilb AR, Wells AM, Hartmann J, *et al*. Nucleus accumbens medium spiny neuron subtypes differentially regulate stress-associated alterations in sleep architecture. Biol Psychiatry 2021, 89: 1138–1149.

49. Oishi Y, Xu Q, Wang L, Zhang BJ, Takahashi K, Takata Y, *et al*. Slow-wave sleep is controlled by a subset of nucleus accumbens core neurons in mice. Nat Commun 2017, 8: 734.

50. Coen CW, Kalamatianos T, Oosthuizen MK, Poorun R, Faulkes CG, Bennett NC. Sociality and the telencephalic distribution of corticotrophin-releasing factor, urocortin 3, and binding sites for CRF type 1 and type 2 receptors: A comparative study of eusocial naked mole-rats and solitary Cape mole-rats. J Comp Neurol 2015, 523: 2344–2371.

51. Itoga CA, Chen YC, Fateri C, Echeverry PA, Lai JM, Delgado J, *et al*. New viral-genetic mapping uncovers an enrichment of corticotropin-releasing hormone-expressing neuronal inputs to the nucleus accumbens from stress-related brain regions. J Comp Neurol 2019, 527: 2474–2487.

52. Muhammad A, Carroll C, Kolb B. Stress during development alters dendritic morphology in the nucleus accumbens and prefrontal cortex. Neuroscience 2012, 216: 103–109.

53. Martínez-Téllez RI, Hernández-Torres E, Gamboa C, Flores G. Prenatal stress alters spine density and dendritic length of nucleus accumbens and hippocampus neurons in rat offspring. Synapse 2009, 63: 794–804.

54. Lewin M, Lopachin J, Delorme J, Opendak M, Sullivan RM, Wilson DA. Early life trauma has lifelong consequences for sleep and behavior. Sci Rep 2019, 9: 16701.

55. Ivy AS, Rex CS, Chen YC, Dubé C, Maras PM, Grigoriadis DE, *et al*. Hippocampal dysfunction and cognitive impairments provoked by chronic early-life stress involve excessive activation of CRH receptors. J Neurosci 2010, 30: 13005–13015.